Assessment of resting state structural-functional relationships in perisylvian region during the early weeks after birth

Roxana Namiranian[1], Hamid Abrishami Moghaddam[1*], Ali Khadem[1], Reza Jafari[2,3], Aimirhossein Chalechale[1]

[1] *Department of Biomedical Engineering, Faculty of Electrical Engineering, K. N. Toosi University of Technology, Tehran, Iran*

[2] *Department of Medical Biophysics, Schulich School of Medicine and Dentistry, University of Western Ontario, London, Ontario, Canada, N6A 5C1*

[3] *Department of Electrical and Computer Engineering, Thompson Engineering Building, University of Western Ontario, London, Ontario, Canada, N6A 5B9*

[*]Corresponding Author:
Hamid Abrishami Moghaddam, Ph.D., Faculty of Electrical Engineering, K.N. Toosi University of Technology, PO Box 16315-1355, Tehran, Iran (e-mail: moghaddam@kntu.ac.ir).

E-mail addresses:
Roxana Namiranian: namiranian.ro@email.kntu.ac.ir
Hamid Abrishami Moghaddam: moghaddam@kntu.ac.ir
Ali Khadem: alikhadem@kntu.ac.ir
Reza Jafari: reza.jafari@uwo.ca

Abstract

This study investigates the structural-functional (S-F) relationships of perisylvian region in the first weeks after birth during rest. Previous joint S-F studies of the perisylvian development were mainly conducted on individual structural and functional features and outperformed non-joint studies. By using a weighted combination of features, a joint S-F study can advance understanding of the perisylvian development in neonates, thereby offering valuable markers for predicting neurodevelopmental disorders. To this purpose, we used 390 structural and 89 functional features for each region of interest (ROI) in perisylvian. Structural features include morphological and myelination features of cortical regions, and functional features include functional connectivity (FC) between each ROI and other brain regions. Subsequently, the S-F hybrid marker for each ROI is produced using the sparse canonical correlation analysis (SCCA). In addition, the significance and consistency of the contribution of each structural and functional feature in the hybrid marker are examined using statistical tests. The findings indicated the correlation between the FC of each ROI with other brain regions, and the myelination of that ROI or other brain regions, while no correlation was observed between the FC and the morphological features of the cortical regions. Furthermore, in the hybrid markers, auditory regions show greater contributions of FC and myelination compared to higher-order regions such as Broca area, suggesting their early development in infants. Additionally, regions such as insula and cingulate gyrus have not only FC but also jointly S-F relationships with most of the perisylvian sub-regions. Therefore, the hybrid markers outperform individual joint markers by introducing additional S-F relationships for characterizing the normal development of the perisylvian region in neonates.

I. Introduction

The perisylvian region of the brain play a crucial role in the processing of language and auditory communication, making them an area of significant interest for researchers studying early brain development. By exploring the structural-functional (S-F) relationships in these brain regions during the early postnatal period, valuable insights can be gained into the fundamental mechanisms that govern language and auditory development in infants. The development of advanced neuroimaging methodologies, such as magnetic resonance imaging (MRI) and functional MRI (fMRI), has provided researchers with non-invasive tools to assess neonatal brain structure and function dynamically. By integrating data from both structural and functional neuroimaging, researchers can achieve a more comprehensive understanding of how the anatomical organization of the brain relates to its function during this critical developmental phase.

The postnatal period coincides with extremely dynamic and rapid brain changes (1,2) which are crucial for understanding how brain evolution influences lifelong cognitive abilities and behaviors (3,4). It is also important for early diagnosis or even prognosis of neurodevelopmental disorders (5,6). However, multimodal (e.g., structural-functional) brain data acquisition and analysis in this period is challenging (7,8) due to neonate's non-cooperativeness, immature brain structure, and inability to respond deliberately to task-based stimuli. Nevertheless, recent advances in neuroimaging and open resource projects such as the developing human connectome project (dHCP) (9) have made available multimodal datasets suitable for structural and functional developmental studies (10–14).

Language and auditory related sub-regions were also of particular interest in most of the postnatal neurodevelopmental studies, because they can be performed without requiring deliberate response of the subjects (15). Accordingly, task based or resting-state functional studies have been performed to examine language and auditory sub-regions and their inter connections with other functional circuits (16–19). The relation between functional connectivity (FC) and language (20,21) and auditory (22–25) performance has been demonstrated using resting-state fMRI (rs-fMRI). Xiang et al. (26) showed that the topology of FC in 6 frontal sub-regions of perisylvian language network during rest, is consistent with the topology of language network of the brain. Nevertheless, few researches have investigated the association between structure and function of auditory and language related regions during rest in early childhood (27–29). Furthermore, when comparing resting-state studies to task-based studies, the data acquisition procedure is typically easier, resulting in larger size datasets. Consequently, the outcomes and models derived from resting-state studies are deemed more reliable.

A few task-based studies attempted to examine structural features for correlation with functional performance in language and auditory regions. Daneshvarfard et al. (30) correlated a microstructural feature of superior temporal gyrus (STG) with latency of auditory response in 17 preterm neonates with gestational age (GA) between 28.4 and 32.2 weeks. Moreover, Adibpour et al. (31) demonstrated that the microstructural measures of inferior frontal gyrus (IFG) modulate the auditory responses in the first 6 months after birth, even after controlling the age. Studies conducted in the first postnatal semester demonstrated the coordination between the myelination of corpus callosum fibers and speed of inter-hemispheric auditory and visual information transfer (31–33). These studies assert the importance of cortical properties in identifying specialized structural features associated with auditory function (31). Morphological features like surface area and folding measures, before term equivalent age, are related to the later language outcome (4,34). Furthermore, the whole brain study on term neonates showed that the cortical thickness is related to the anterior-to-posterior gradient of resting-state FCs (10). However, to the best of our knowledge, no study has been conducted to determine whether shape-related cortical features are significantly correlated to functions of auditory or language-related regions, during first few weeks after birth.

Former neonatal joint S-F studies on language and auditory regions investigated the relation between individual functional and structural features (30,31,33). They did not explore whether a combination of structural features may be associated with a mixture of functional measures. For example, the joint

study in (30), showed that maturation of the auditory responses is correlated with myelination of auditory pathways and regions, while after controlling for the age they become uncorrelated. Another joint analysis (31) failed to find the link between functional lateralization in auditory responses and structural asymmetries, while asymmetric maturation of perisylvian sub-regions and pathways (35,36), are consistent with the language auditory laterality (37–40). These findings are in accordance with the fact that there are complex relationships between brain structure and function (41), and that more informative structural and functional features are required to comprehend the links. Hybrid features in both the structural and functional sides are hypothetically more promising than single ones to understand complex S-F couplings.

It is worth noting that joint studies seek to identify comprehensive structural features that can better predict brain function (10,31). Such biomarkers can be used effectively for early diagnosis at ages when cognitive impairments symptoms have not yet appeared or functional measures are difficult to acquire. While joint S-F analysis facilitated the diagnosis of language and neurodevelopmental disorders during adulthood (42–44), such joint studies have not been conducted on neonates yet. Zhang et al., (14) discovered atypical patterns of S-F couplings in premature birth. Further studies with a thorough investigation into hybrid and innovative structural and functional features, can provide comprehensive information (5,45) about the normal maturation of the brain. These studies are essential for the early diagnosis of diseases.

To address the aforementioned issues, we utilized MRI and rs-fMRI and adopted a feature extraction approach to investigate functional and structural features of language related regions involved in the normal S-F relationships during the first few weeks after birth. Specifically, we focused on examining the FC patterns and structural features of these regions during rest. We also used sparse canonical correlation analysis (CCA) (46), a data-driven multivariate method, to simultaneously capture comprehensive linear interactions between multiple structural and functional measures of the brain. The incorporation of sparsity terms in the CCA algorithm enables effective handling of high-dimensional data, addressing concerns of overfitting and lack of interpretability that conventional CCA may suffer from. Consequently, features are selected based on the association between the two modalities, promoting joint information extraction rather than treating each modality separately (10,14). The results obtained from our analysis demonstrate that new hybrid structural features correlate with hybrid functional measures, revealing the relationships between regional structural features and FCs in perisylvian sub-regions.

The remaining sections of the paper are structured as follows: Section II outlines the materials and methods used, encompassing the neonatal datasets for structural and functional MRI. It also presents the proposed pipeline including preprocessing, feature generation, sparse CCA, as well as statistical analysis. Section III showcases the results, including the extracted hybrid S-F markers. In Section IV, the results are discussed in terms of their alignment with previous relevant studies. Finally, the concluding remarks are given in Section V.

II. Materials and Methods

Neonatal dataset

The neonatal neuroimaging dataset released by dHCP (47) was employed in this study. This dataset provides multi-modal neuroimaging (functional, structural and diffusion MRI) sessions comprising around 500 neonates aged from 24 to 45 weeks GA in the second release (see http://www.developingconnectome.org for more details). In our study, only term neonates with the birth age greater than 37 weeks GA were participated. After excluding the subjects with missing one of the structural or functional data, and subjects with miss-registration, a final set of 267 sessions was enrolled to investigate the structural and functional relationships (124 girls and 143 boys, age-range: 37.43- 44.71, mean age ± STD: 41.00±1.68 weeks GA). All neonates were scanned during natural sleep on a 3T Phillips Achieva with a dedicated neonatal imaging system and a neonatal 32 channel phased

array head coil at the Evelina Neonatal Imaging Centre, St Thomas' Hospital, London. Hearing protection was provided for infants.

Anatomical MRI was acquired using a turbo spin echo (TSE) sequence for T2w and an IR (inversion recovery) TSE sequence for T1w images, in sagittal and axial slice stacks (in-plane resolution 0.8 × 0.8 mm^2 and 1.6 mm slices overlapped by 0.8 mm). Other parameters were–T2w: TR/TE = 12000/156 ms; T1w: TR/TI/TE = 4795/1740/8.7 ms. Final resolution of reconstructed structural images, using slice-to-volume registration was 0.5 × 0.5 × 0.5 mm^3 (for more details check (48)).

Resting-state fMRI using multiband (BM) 9× accelerated echo-planar sequence with 2.15 mm isotropic resolution (TE/TR = 38/392 ms) was performed for infant brain during 15 min. In addition to the main EPI scans, single-band EPI reference scans were also obtained with a readout bandwidth matching the main scans. Additional spin-echo EPI scans were acquired with phase-encoding directions of 4xAP and 4xPA. The reconstructions were performed using the extended SENSE framework described by Zhu et al. (49), with sensitivity maps calculated from the corresponding single-band data. Field maps were obtained using an interleaved spoiled gradient-echo sequence with dual TE (TR= 10 ms, TE1= 4.6 ms, TE2=6.9 ms, a flip angle =10°), an in-plane resolution of 3 mm isotropic, and a slice thickness of 6 mm (for more details check (50)).

The proposed pipeline

The proposed pipeline for extracting and assessing the interplay between structure and function of the neonatal brain is shown in **Fig. 1**. First, in data processing and feature generation block, the brain is parcellated into 90 regions using the AAL atlas. For each region, 5 structural features were derived and the FCs between the regions of interest (ROIs) and other regions defined by the AAL atlas were computed. Structural and functional features are used to generate hybrid S-F markers by employing the SCCA technique. To evaluate hybrid markers or canonical weights, the statistical analysis was employed on resampled structural and functional features. Finally, features with significant and consistent nonzero canonical weights were chosen based on the statistical results and the main canonical weights obtained from the SCCA technique. The subsequent sections will delve into the details of this pipeline.

A. Dataset processing and feature generation

The neonatal brains were parcellated to perisylvian sub-regions using UNC atlas (51). UNC, also known as neonatal AAL atlas, is a volumetric infant brain atlas proposed for 3 age-ranges including neonates, 1- and 2-years old infants. Among 90 regions of AAL atlas, the perisylvian sub-regions are as follows: triangular gyrus (trianG), opercular gyrus (operG), supramarginal gyrus (suprG), angular gyrus (AG), STG, medial temporal gyrus (MTG), heschl's gyrus (HG), and insula in both hemispheres. The labelled ROIs of AAL were propagated to the 40-week templates based on multi-channel registration (48). Age-specific AAL ROIs were linearly and then nonlinearly registered to the structural space defined by T2w image of each participant. Volumetric ROI masks were used for functional data processing. These registered masks of each AAL ROIs were mapped to the neonate's cortical surfaces using Connectome Workbench from HCP tools (https://www.humanconnectome.org/software/connectome-workbench), and served for structural processing.

– *Structural data processing*

The structural MRIs undergo some preprocessing steps, including motion and bias correction, as well as brain extraction via the structural dHCP pipeline. Subsequently, cortical surfaces of each neonate are extracted using DrawEM algorithm (52). Next, the structural dHCP pipeline is used to estimate individual surface feature maps for 4 features including myelination measure and various morphology features such as mean curvature, sulcal depth, cortical thickness (48). The surface feature maps provided by dHCP team are averaged over the vertices of each parcel of surface registered AAL atlas. The surface area of each ROI is another structural measure that was computed to model the inter-subject variations

of neonatal brains. Twelve subcortical and deep gray matter regions were excluded from ROIs. As a result, structural features consist of 390 features (5 structural features of 78 ROIs) from 267 neonates.

– *Functional data processing*

The preprocessing procedures, including motion correction, super-resolution reconstruction and cortical surface reconstruction using the Medical Image Registration ToolKit (MIRTK) specifically adapted for neonatal MR data (48,53) were applied to T1w and T2w images. For the rs-fMRI, the preprocessing involved correction for geometric distortions and head motion, registration to T2w structural images, band-pass filtering (150 s), and ICA denoising (50). The volumetric AAL labeled masks from each T2-space was transformed to functional space (using transformation matrices provided by dHCP team). Then, FCs were calculated between each pair of brain regions using Pearson correlation (54,55) between regional time series that are extracted from 90 ROIs by averaging the fMRI signal within each region.

We regressed out age from structural and functional feature sets to ensure that age, as a potential confounder of features, does not drive the correlation.

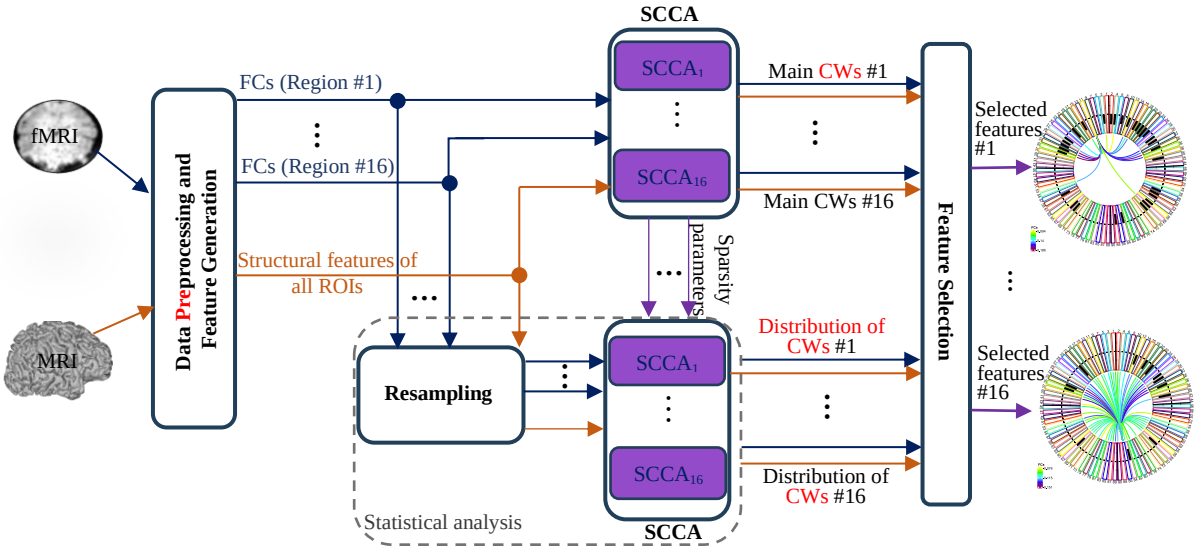

Fig. 1 *The proposed pipeline for extracting correlated structural and functional biomarkers. Initially, in the data preprocessing and feature generation stage, the brain is divided into 90 regions using the AAL atlas. Structural features including morphological and myelination features are extracted for each brain region. The functional features extracted for each ROI include the FCs between that ROI (labeled by number 1 to 16) and other regions. In the second stage, by employing the sparse CCA (SCCA) technique, the hybrid S-F markers are generated using the appropriate sparsity parameters. Next, to assess the canonical weights (CWs), statistical analysis is applied to the resampled structural and functional features. Finally, significant and consistent non-zero canonical weights are chosen based on the statistical findings and the primary canonical weights of the original data.*

B. Sparse CCA (SCCA)

To identify correlations between structural and functional data, we used SCCA, a CCA algorithm adapted for high-dimensional data which incorporates feature selection by embedding lasso penalty in CCA approach. Like CCA, that provides shared latent space (canonical variates) that maximizes the correlation between the two datasets, SCCA correlated datasets using sparse linear projection of both sets (canonical weights). SCCA can be expressed as an optimization problem:

$$\max_{\boldsymbol{u},\boldsymbol{v}} \ \boldsymbol{u}^T\boldsymbol{X}^T\boldsymbol{Y}\boldsymbol{v} \ \text{ subject to } \boldsymbol{u}^T\boldsymbol{X}^T\boldsymbol{X}\boldsymbol{u} \leq 1, \boldsymbol{v}^T\boldsymbol{Y}^T\boldsymbol{Y}\boldsymbol{v} \leq 1, \|\boldsymbol{u}\|_1 \leq \lambda_1, \|\boldsymbol{v}\|_1 \leq \lambda_2 \qquad (1)$$

which finds loading vectors, $\boldsymbol{u}_{p\times 1}$ and $\boldsymbol{v}_{q\times 1}$ that maximize $cor(\boldsymbol{X}\boldsymbol{u}, \boldsymbol{Y}\boldsymbol{v})$. $\boldsymbol{X}_{n\times p}$ and $\boldsymbol{Y}_{n\times q}$ represent FCs of each perisylvian sub-region ($p = 89$) and structural features of ROIs of AAL atlas ($q = 390$), respectively, with the same number of subjects in rows ($n = 267$). The sparsity is achieved by applying lasso penalties, which needs to be tuned using grid search between ranges of λ_1 and λ_2 parameters, from

0 to 1 in increments of 0.1. We employed the penalized multivariate analysis (PMA) package in the R programming language to implement the SCCA algorithm proposed by Witten et al. (56).

As stated in the SCCA section in **Fig. 1**, the SCCA algorithm was individually applied to each of the 16 perisylvian sub-regions, and the resulting sparsity levels and the coefficients of the features that exhibit the highest correlation, were computed. The determination of appropriate sparsity levels, denoted as λ_1 and λ_2, has been a challenging task, extensively explored in previous studies. Permutation test is commonly utilized for estimating the sparsity levels of canonical vectors (57,58). This method was also employed by (56) to select a significant sparsity level. In this approach, significance of each sparsity level in grid search is determined by comparing the canonical correlation (CC) of the original data with the CC of randomly associated data. The benchmark is set based on the CC of the original data surpassing that of the randomly related data. Given the crucial role of the CC in this process, a more accurate estimation is achieved by utilizing the jackknife technique to estimate the CC, rather than relying just on the original data. Therefore, Algorithm 1 presents SCCA as depicted in **Fig. 1** (top), utilizing the original data. In Algorithm 1, the notation "-i" for a data matrix, represented as $\mathbf{X}[-\mathrm{i},:]$, refers to excluding the i-th row corresponding to i-th individual. "Sample(n)" denotes the selection of n random numbers between 1 and n without replacement. Hence, a criterion for determining the appropriate sparsity level for the structure and function is that the p-value should be less than 0.05. Recent studies conducted by Yang et al. (59) on the CCA algorithm have revealed that low CCs lead to unstable outcomes, while selecting higher CCs enhances significantly the result's stability. Therefore, apart from statistical significance, another criterion involves selecting the sparsity level with the highest CC as the appropriate level of sparsity. Therefore, the outcome of Algorithm 1 involves the sparsity level and canonical weights based on significant correlation with maximum CC.

Algorithm 1:

Input: a sequence of structural and functional sparsity ($\mathbf{L}_{\mathbf{Sseq}}$, $\mathbf{L}_{\mathbf{Fseq}}$), structural data $[\mathbf{X}]_{\mathrm{n}\times\mathrm{p}}$, functional data $[\mathbf{Y}]_{\mathrm{n}\times\mathrm{q}}$

Output: functional and structural sparsity and canonical weights (u,v)

Initialize: permutation number
For each structural sparsity value (l_s) of sequence $\mathbf{L}_{\mathbf{Sseq}}$
  For each structural sparsity value (l_f) of sequence $\mathbf{L}_{\mathbf{Fseq}}$
    For each subject (i)
      $cc[i] = SCCA(\mathbf{X}[-\mathrm{i},:], \mathbf{Y}[-\mathrm{i},:], l_s, l_f)$
    End
    $\boldsymbol{CC}\ [l_1, l_2] = mean(cc)$
    For j = 1:permutations number
      $\mathbf{X}_{perm} = \mathbf{X}[sample(n),:]$, $\mathbf{Y}_{\boldsymbol{perm}} = \mathbf{Y}[sample(n),:]$
      $\mathbf{cc}_{perm}[j] = SCCA\ (\mathbf{X}_{perm}, \mathbf{Y}_{perm}, l_s, l_f)$
    End
    $Pvalue[l_s, l_f] = mean(\mathbf{cc}_{perm} > \boldsymbol{CC})$
  End
End
$\lambda_1, \lambda_2 = which(max(\boldsymbol{CC}), Pvalue < 0.05)$
$u, v = SCCA(\mathbf{X}, \mathbf{Y}, \lambda_1, \lambda_2)$
Return $\lambda_1, \lambda_2, u, v$

C. Statistical analysis and feature selection

Apart from selecting significant CCA components, examining the stable and significant coefficients are also important. Therefore, the next stage involves examining the coefficients using the bootstrap method, as depicted schematically in the SCCA in statistical analysis section of **Fig. 1** (bottom). In this

method, the data is sampled with replacement, 500 times. In each iteration, n subjects are selected, considering that the number of subjects is crucial in the processing and may influence the results. Then, based on the predetermined sparsity level from the previous step, the SCCA algorithm is applied to each set of 500 datasets, and the coefficients corresponding to structural and functional features are obtained. The obtained coefficients are subject to a statistical test to assess their significance. This test employs a criterion that involves comparing the coefficients derived from bootstrapping with those obtained from the original data. The criterion includes performing a t-test and calculating the False Discovery Rate (FDR) to identify coefficients that exhibit statistical significance ($q>0.05$). Moreover, coefficients that fall outside the range of the 95% confidence interval in the bootstrap tests are deemed unsuitable. Additionally, coefficients with a 95% confidence interval overlapping with zero are considered as zero. Furthermore, the coefficient of variation is computed, and coefficients with a variation-to-mean ratio of less than 20% are regarded as appropriate.

III. Results

We investigated the relationship between the 5 structural features of whole brain regions with the FCs between all brain regions and 16 perisylvian sub-regions, separately. We sought to identify hybrid structural and functional biomarkers that would allow us to extract the strongest relationship between structure and function.

The SCCA performance was first contrasted with the correlations of the individual structural and functional features using Pearson correlation. The correlation between the individual structural and functional features and the proposed hybrid S-F markers was shown in **Fig. 2**. The distribution diagrams indicate significant univariate correlations between different structural features and FC of each presylvian sub-region and other ROIs. The red bar in each diagram represents the estimated correlation between the proposed hybrid S-F markers using bootstrapping. As illustrated in **Fig. 2**, the hybrid S-F markers extracted by SCCA show larger correlations than individual features. It is noteworthy that in contrast to the correlations of individual features, the resulted SCCA correlation is conventionally a positive value (according to equation 1). In other words, the individual features with negative correlation are particularly weighted so as to contribute as positive correlation in the hybrid marker. The details of the 10 most significant correlations of individual structural and functional features of each perisylvian sub-region are presented in Table 1 in Supplementary materials. The regional correlation maps are also presented in **Fig. S1** in supplementary materials. It shows the regions with significant S-F correlation for each structural feature separately. According to the distribution of significant regional relations between structure and function for each structural feature (see **Fig. S1** in supplementary materials), the T1w/T2w ratio, as a myelination index, establishes the strongest correlation with FCs. Based on the univariate analysis, myelination is the most correlated structural feature to FCs also in regions with jointly related structure and function.

It is noteworthy that the negative and positive correlation between individual structural and functional features in **Fig. S1** are mainly consistent with previous studies. The previous studies demonstrated the positive correlation between myelination and FC, which shows the development of myelination causes stronger FCs (10). Various factors including neuronal migration to gray matter and programmed cell death with different timing for each region cause various regional developmental pattern of surface morphology around birth (60). Consequently, different patterns of S-F relation are expected when considering all regions. Mostly negative correlations between cortical thickness and FC are consistent with previous findings in (10). The observed positive and negative relation between FC and sulcal depth and curvature are in line with previous studies of cortical folding. For example, the relation between sulcal depth and long-range FC is positive, while its relation with local FC is negative (61).

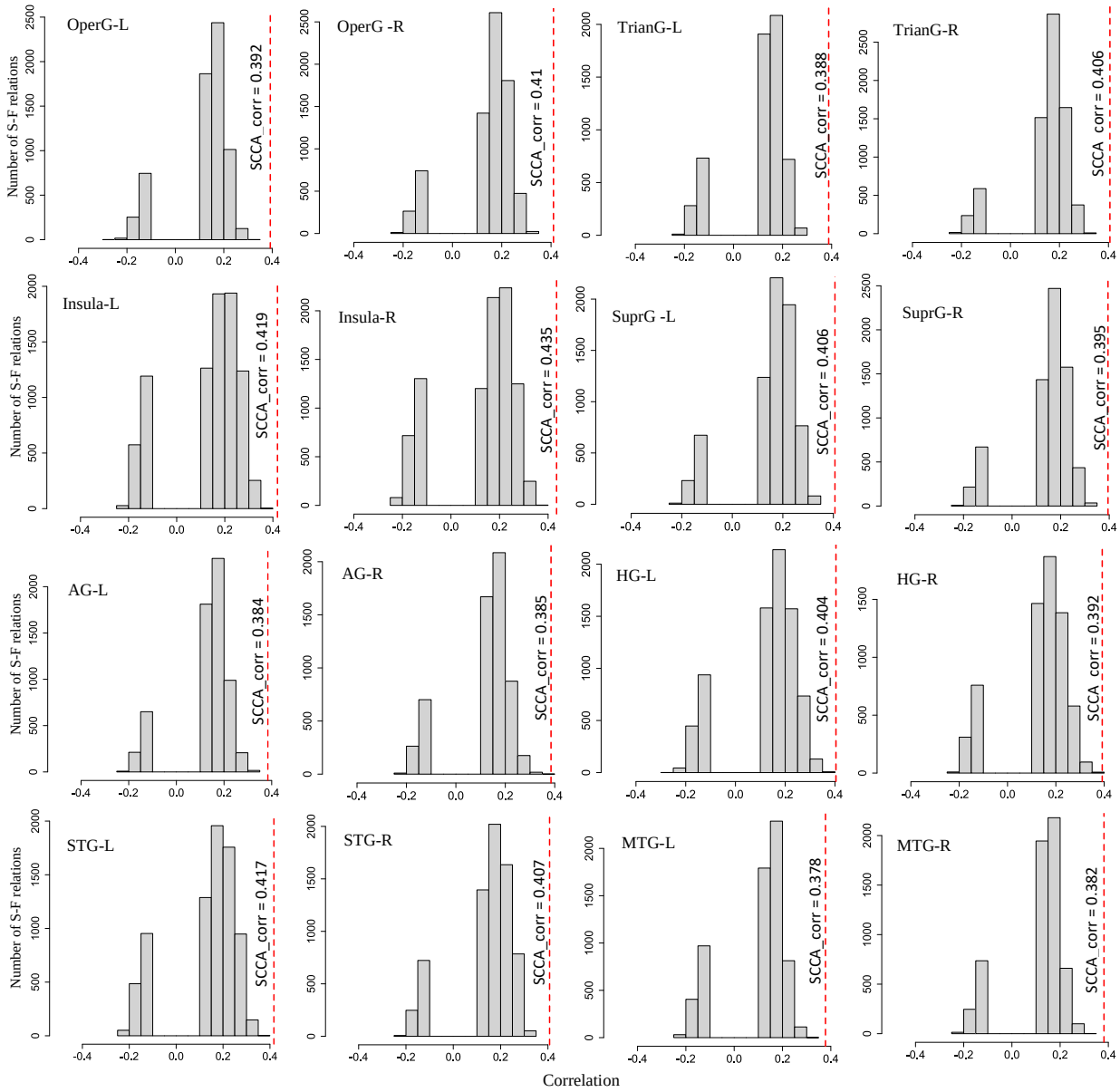

Fig. 2 *Univariate and SCCA performance in S-F correlations. The bar plots illustrate the distribution of linear correlation coefficients of all individual structural features and FC between the specified perisylvian ROIs and all brain regions. The red line in each diagram specifies the estimation of correlation coefficient between the proposed hybrid S-F markers using bootstrapping. TrianG: triangular gyrus, OperG: opercular gyrus, SuprG: supramarginal gyrus, AG: angular gyrus, STG: superior temporal gyrus, MTG: medial temporal gyrus, HG: heschl's gyrus, L: left, R: right*

The first following part of the results indicates how structural and functional features contribute to the S-F coupling for each of the 16 regions. The second part demonstrates the relationships between other brain regions and the perisylvian sub-regions.

Significant and consistent coefficients in perisylvian S-F relations

The coefficients of structural and functional features that have a significant and consistent role in creating S-F markers in 16 perisylvian sub-regions are shown in **Fig. 3**. In **Fig. 3**, only the values for significant and consistent coefficients are shown and the coefficients that were not selected in the statistical test were set to zero. The circular diagrams in this figure specify 90 AAL regions separately for the right hemisphere in the right half of the circular diagram and for the left hemisphere in the left half of the diagram. Inside each diagram, you can see the FC between regions, with respect to each perisylvian sub-region as seed. There is a bar graph around that shows the canonical weights of

structural features. Details of the results, such as the selected sparsity level and canonical correlation obtained by the Jackknife method, the 95% confidence interval of the bootstrap test, the main coefficients of original data, and the results of the statistical tests are provided in supplementary materials.

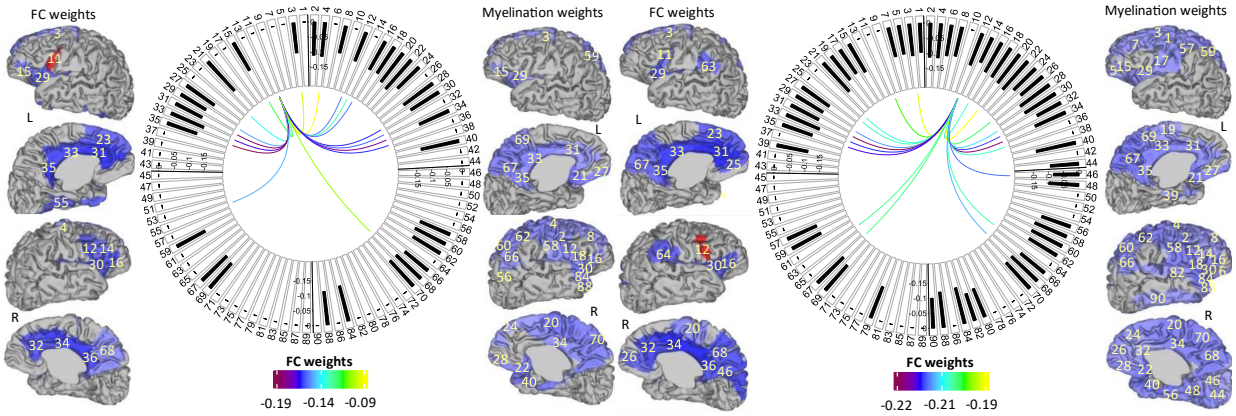

Opercular-L, correlation=0.28 Opercular-R, correlation = 0.32

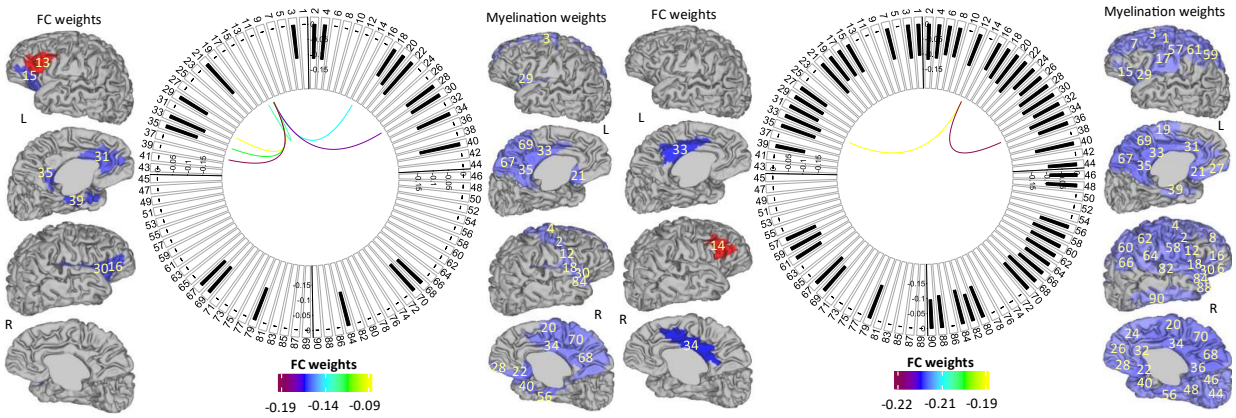

Triangular- L, correlation = 0.29 Triangular-R, correlation = 0.29

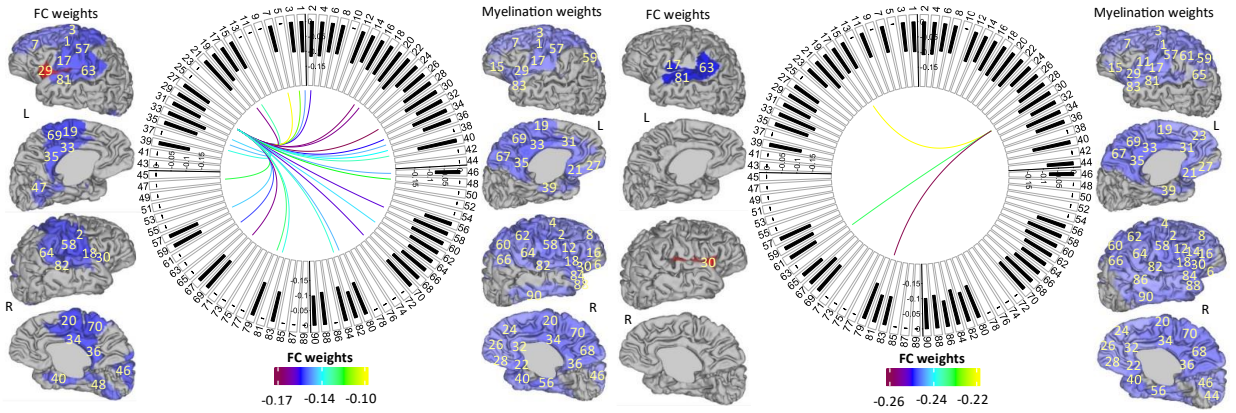

Insula-L, correlation = 0.34 Insula-R, correlation = 0.35

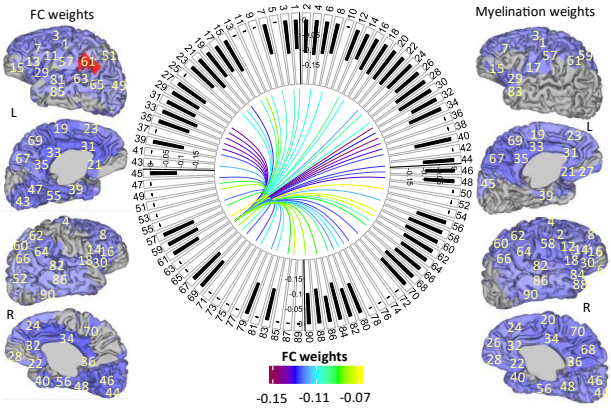

Supramarginal gyrus-L, correlation = 0.31

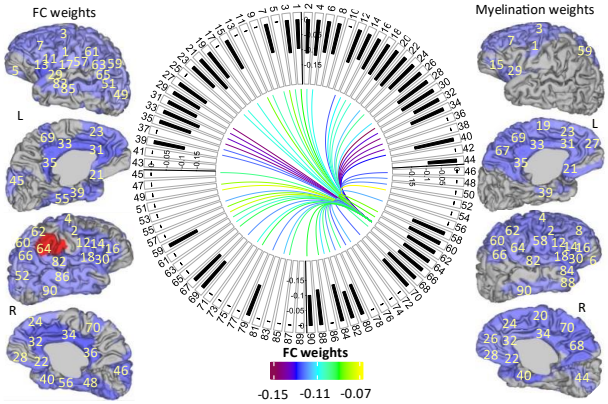

Supramarginal gyrus-R, correlation = 0.30

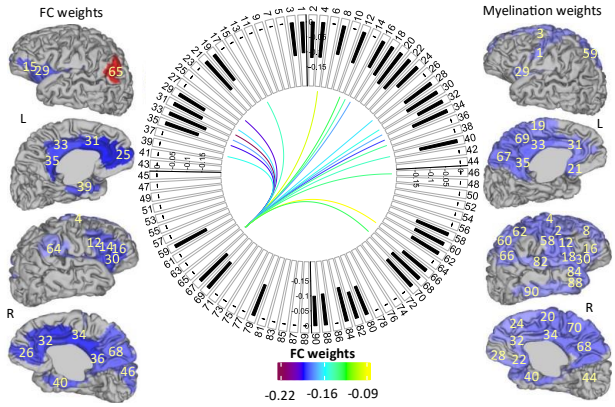

Angular gyrus-L, correlation=0.30

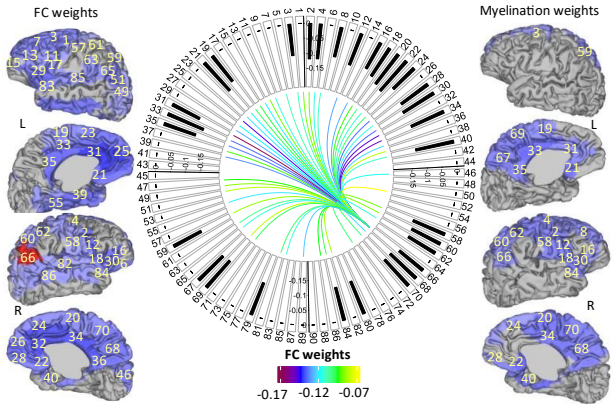

Angular gyrus-R, correlation=0.28

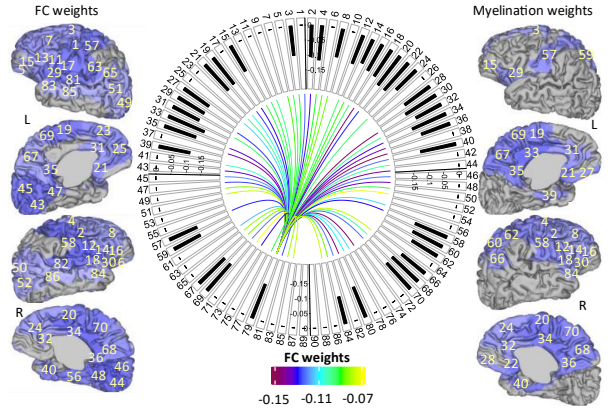

Heschl gyrus-L, correlation = 0.31

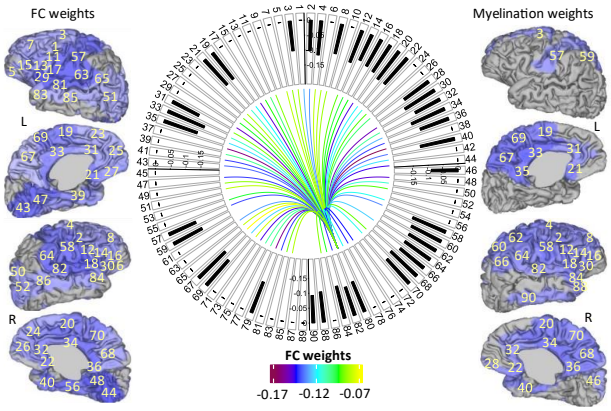

Heschl gyrus-R, correlation = 0.29

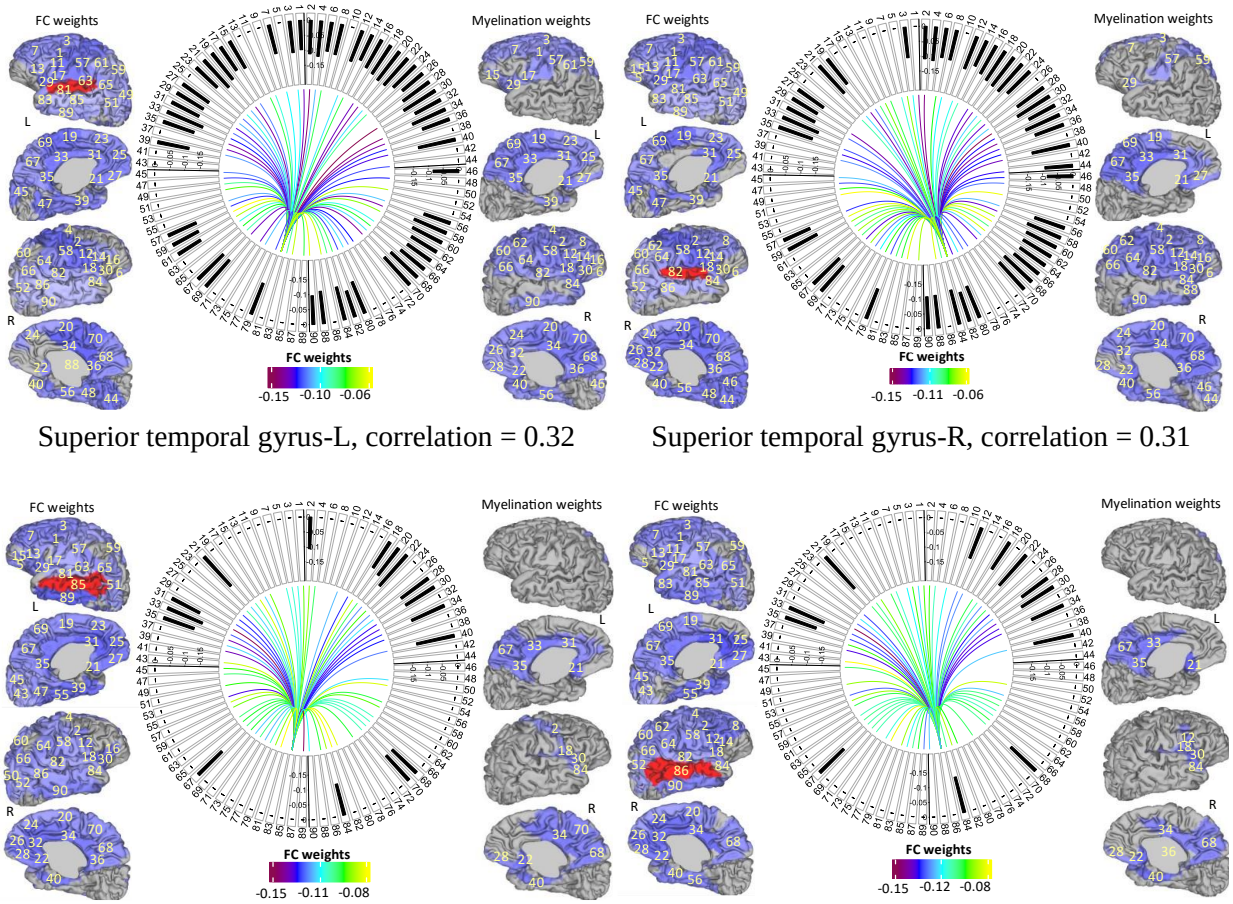

Fig. 3 *Significant and stable canonical weights of myelination and FC contributed in correlated S-F markers. The connections within each circle show the FCs between the specified perisylvian seed and other brain regions. The color of each connection corresponds to the canonical weight of the FCs. The black bar plots around the circle indicate the canonical weights of myelination. The brain maps visualize the canonical weights of structural and functional features of the brain regions. As the absolute values increase, the color gradually intensifies, transitioning from a lighter tone to a darker hue (dark blue corresponds to the value of -0.2). The specific perisylvian ROI is shown in red color.*

Our findings using all structural features (details in Supplementary materials), show that the myelination feature contributes mostly in constructing composite structural marker related to functional markers in terms of stability and significance. Therefore, in **Fig. 3**, other structural features including cortical thickness, curvature, surface area and sulcul depth are considered as zero and not shown. Additionally, **Fig. 3** shows that auditory-related areas and Wernicke's areas (supramariginal and amygdala) have more significant and consistent S-F couplings than the insula and Broca's areas (triangular and opercular).

To investigate more specifically the relationship between morphological features and FCs, we reiterated the pipeline by excluding myelination, which was the only correlated feature with FC after statistical analysis. The results using Algorithm 1 did not show significant sparsity for all regions, except for certain perisylvian sub-regions such as opercular, insula, STG, left supramarginal gyrus and left heschl's gyrus. However, the statistical analysis showed no consistent and significant relation between the morphological features and FC. The supplementary files (**Fig. S18** to **Fig. S25**) contain the results of the statistical tests and corresponding canonical weights.

The degree of involvement of AAL regions in hybrid S-F markers

The contribution of each brain region in all 16 hybrid S-F markers is ranked into four categories based on their canonical weights as shown in **Fig. 4**. The first category (**Fig. 4** (a)) represents the regions with joint S-F contribution, whose myelination and FC with perisylvian ROIs participate in S-F markers.

The second category (**Fig. 4** (b)) represents region with functional contribution, whose FC with perisylvian ROIs participate in functional markers but their myelination does not contribute in structural markers. The third category (**Fig. 4** (c)) represents the regions with structural contribution, whose myelination involve in structural markers but there is no contribution of their FC with perisylvian ROIs in functional markers. The last category (**Fig. 4** (c)) represents regions with no contributions, in which neither myelination nor FC between perisylvian ROIs and these areas involve in structural markers and functional markers, respectively. The color of each region in **Fig. 4** indicates the number of structural and/or functional markers in which these regions contribute. For example, in **Fig. 4** (a), the STG of the left hemisphere is blue and equal to the value of 10, which shows that both the myelination of the STG region and its FC with perisylvian sub-regions contribute, respectively, in 10 S-F markers.

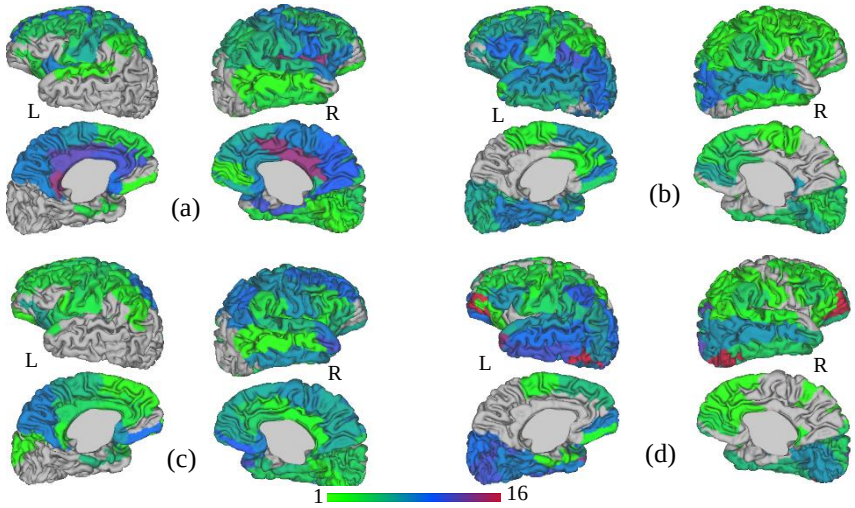

Fig. 4 *structural and functional contributions of all brain regions. (a) regions with joint S-F contribution (b) regions with functional contribution (c) regions with structural contribution (d) regions with no contribution*

The obtained results indicate that in the insula (especially the right hemisphere), the sub-regions of the cingulate gyrus, the superior frontal gyrus of the left hemisphere, the percuneus, the parahipocampus gyrus, and the right olfactory region, structurally and functionally contribute in creating an S-F relationship. Also, in general, the regions of the right hemisphere can be considered more prominent in creating a connection between the structure and function of the brain.

The FCs between the perisylvian sub-regions and the occipital regions can be considered as connections that contribute in the creation of functional ~~bio~~markers, while the structural features of these regions do not participate in the related-structural marker with appropriate weights.

The orbitofrontal cortex (middle) and inferior occipital gyrus of both hemispheres are the areas that did not have a significant and consistent role in this study neither structurally nor functionally.

It should be noted that the structural features of the hippocampus, the amygdala, the caudate, the putamen, the Pallidum and the thalamus were not participated in analysis because the extracted structural features were related to the cortical areas of the brain. Therefore, as expected, these regions placed in the category of areas where only their functions contribute. Except for the Amygdala, which is only connected to the Heschel's gyrus, other subcortical and deep areas of the gray matter are connected with several perisylvian areas, in such a way that these connections involve in creating a functional marker related to the structure.

IV. Discussion

The value of S-F approach to study brain aging and disorders have been demonstrated by recent investigations. Zimmermann et al. illustrated that the age-related S-F association can provide additional insights into brain aging beyond what can be revealed by each modality alone (62). Furthermore, Rudie et al. (63) used a similar approach to show that social and communication symptom severity of autism

spectrum disorder (ASD) are associated with an imbalance of global and local efficiency between structural and functional networks. Accordingly, the S-F approaches are potentially promising to provide predictive biomarkers for early diagnosis or prediction of brain and behavioral disorders. Jiang et al. investigated the decrease in S-F coupling to predict suicide attempts in bipolar patients (64). Likewise, Wen et al. (65) discovered the link between global increase in S-F coupling as well as within specific brain modules and decreased dynamic brain function in Tourette Syndrome (TS). They also found that the S-F correlation could serve as a biomarker for early diagnosis of TS.

Establishment of the S-F atlas of normal brain development, may help prediction or early diagnosis of brain or behavioral disorders. The early postnatal period is crucial for investigating brain development, since the brain undergoes fundamental changes and any deviation from normal growth can yield to subsequent structural or functional disorders. A few S-F studies tried to model the neonatal brain development in preterm and term subjects (10,11,14,30,31). The objective of this study was to improve the present understanding of the S-F relationships by utilizing a large sample size of term infants. Similar to most of the previous early neurodevelopmental studies (30,31), this study was focused on perisylvian sub-regions because they can be investigated via passive responses of the subjects to auditory and language stimulations. However, we examined hybrid S-F markers as an alternative to individual S-F features which were previously studied.

Previous S-F studies have identified some significant S-F relationships of the neonatal perisylvian sub-regions using individual features. However, after controlling for the effect of age, only few structural changes of the brain remained significantly correlated with the function (30,33). This was may be due to using individual structural and functional features. With this perspective, we examined the S-F relationship using hybrid S-F markers after regressing out the effect of age. The rs-fMRI studies of the similar age-range using various structural and functional features, detected some correlations between structure and function of the brain (10,14). The whole-brain results showed the S-F relation during rest had promising results in modeling the maturation difference between preterm and term neonates (14) and explored some consistent and generalizable structural markers related to functional gradients (10) for term neonates. However, they didn't control for the age effect.

The first component of SCCA in our age-controlled S-F analysis, showed stable and significant relations between myelination and FCs of different regions. Recently, Larivie`re et al. (10) showed T1w/T2w intensity has significant relation with principal functional gradient in 40 term neonates. Similarly, the myelination was related to rest-state homotopic FCs in term and preterm neonates in (11). Compared to morphological features, the microstructural measure showed the strongest relationship to the spatial variations in cortical gene expression throughout gestation (66). Although myelination has not been compared to morphological features in earlier S-F studies, this relationship has always been taken into consideration based on physiological evidence linking the development of neuronal pathways and their myelination with their function (30,31,67). In our study, the univariate findings also confirmed the strong coupling between myelination and FCs. Additionally, if myelination is used as structural feature, more regions will be jointly correlated with their FCs. Larivie`re et al. (10) also showed a correlation between the cortical thickness and second principal functional gradient of the posterior to anterior regions. On the other hand, cortical thickness showed no significant relation with homotopic FCs in term and preterm neonates (11). Our study showed no significant association between FCs and morphological features. Hypothetically, considering other significant canonical components may reveal the relation between morphological features and FCs. However, our additional analysis using only morphological features and FCs showed no correlation. The discrepancy between our result and the results presented in (10) on morphological features, may be due to regressing out the age. In addition, the S-F investigations demonstrated a positive association between the growth of neuronal networks and myelination and an improvement in FCs (10,14,65). Similar to earlier studies, our results also show that myelination and brain function change cooperatively. The CCs of the first component are positive, and the canonical weights of myelination and FC are consistent and supporting each other.

Consistent with previous task-based fMRI and DTI studies (68,69), here hybrid functional markers of temporal cortex have a larger number of significant FCs weights with respect to opercular and triangularis regions. The language dorsal pathway that connects superior temporal cortex to motor regions develop earlier than the pathway that connects temporal cortex and Broca areas which concern sentence syntax processing (68,69). Our results show pericentral regions contribute structurally and functionally with most of the perisylvian sub-regions notably STG, Heschl's gyrus and MTG. The sensory-motor connection contributes to early language development during the first months of life by providing bidirectional feedback during the babbling phase (69,70).

There is a bilateral FC between Heschl's gyrus and auditory, sensorimotor, cingulo-opercular, and visual networks in old adults during rest (71). Our results show similar patterns of FC in both hemispheres within the first months after birth. Additionally, the myelination of these regions contributes to the hybrid structural marker. The FCs between Heschl's gyrus and cingulo-opercular network support the auditory attention processes. They are correlated with the hearing ability and uncorrelated to the age or cognitive performance (71). Therefore, the connectivity of cingulo-opercular network with auditory regions is suspected to be the result of recruiting attentional cognitive resources in adults with hearing loss (71–73). It is believed that the Heschl's gyrus FCs are supported structurally and formed in the early stages of development.

The insula is a major afferent hub that receives extensive viscero-autonomic feedbacks, while the cingulate gyrus performs as an efferent hub responsible for generating relevant visceral, autonomic, behavioral, and cognitive responses (74,75). Their role as hub regions is supposed to begin during neonatal period (76). These two areas belong to the salient network that stablishes the coupling with the auditory network in preterm neonates (77). The structure of cingulate gyrus, at birth, is an important predictor of language, cognitive and motor performance in the following months (78). Cingulate gyrus and insula contribute structurally and functionally to the S-F hybrid markers. It demonstrates that their connectivity with other well-developed auditory and language regions is consistent and significant. However, when the insula is used as seed for analysis, fewer significant FCs and S-F relationships are observed compared to other perisylvian sub-regions. This may be due to the immaturity of connections in higher cognitive regions compared to sensory-motor regions in neonates (8,36).

Using SCCA method to extract hybrid S-F markers has two advantages. First, it enables us to explore multi-dimensional S-F space to find correlations stronger than what individual S-F features provide (30,31). Second, it looks for a sparse and optimal subspace in which a combination of selected features establishes the S-F relationship. It is noteworthy that components' selection in CCA is based on their S-F correlation rather than their canonical weights. It has been shown that high CCs are crucial for the stability of the canonical components (59). Recently, false discovery rate of canonical weights (79) is being considered to replace the CCs in SCCA. In our approach, like (58), the significant components and stable weights were selected based on CCs and bootstrapping test, respectively. However, the features removed by bootstrapping test may reduce the correlation between the remained significant S-F markers.

V. Limitations and future works

The relatively small sample size of neonates compared to the data dimension was one of the limitations of our study. Despite the use of sparse parameters to mitigate this limitation, a larger number of participants would improve the generalization of the resulted markers. Additionally, the inclusion of diverse populations across various ages allows for a more comprehensive investigation of S-F relations.

Our study being focused on examining the S-F relationship in normal subjects, we enrolled only term infants. It is crucial to consider the infants' health beyond the immediate post-birth period and conduct longitudinal studies. The availability of longitudinal health data for the neonates participating in our study would prevent infiltration of the suspicious subjects and improve our model of the S-F

relationships in a healthy brain. Obviously, the excluded subjects may serve as test samples in order to assess the prognosis ability of the created S-F marker.

Like the previous neonatal S-F studies (11,14,30,31), we did not take into account the gender of neonates. The sex difference of the neonatal brain is believed to be limited, because of the restricted differential sex chromosome expression and weak production of sex hormones during early stage of development. Nevertheless, inconsistent results of structural and functional studies show limited sex-based differences in neonatal brain (5,80). There is no evidence on the neonatal sex differences of cortical thickness and global gyrifications (81–84). Sex-related differences of microstructural measures are still unknown (5,85). Some regional sexual dimorphism in brain size have been reported in the early stages of development (86–89), while there are no significant sex-based differences of the global brain volume (90,91). Recently, some perinatal sex-related differences of FC patterns were demonstrated (92–94). Further investigations may help to reveal the effect of gender on neonatal hybrid S-F markers.

This study developed hybrid S-F markers, considering the linear S-F association. However, recent studies demonstrated the potential of non-linear models like deep neural networks to reveal more complex S-F relationships (95,96). Moreover, there are a number of functional (e.g., amplitude of low-frequency fluctuations (ALFF)) and structural (e.g., structural connectivity) features that were not considered in our study. Future studies using non-linear models and a variety of structural and functional features may help to achieve a comprehensive S-F marker during brain development.

Some structural and functional asymmetries in perisylvian sub-regions have been reported by previous studies during perinatal period (69,97–100). It seems that there are some differences in S-F markers between the left and right perisylvian sub-regions in our study. Further studies should be conducted to investigate the significance of laterality of the neonatal S-F associations.

In this study, we used concurrent changes of structure and function of subjects to extract the S-F couplings. Further studies may be performed to investigate correlations between asynchronous structural and functional features of different ages, in order to explore the lead/lag development of the structure versus function.

VI. Conclusion

In this study, we proposed hybrid S-F markers for the perisylvian sub-regions in neonates by integrating various features extracted from functional and structural MRI data using SCCA. This method addresses the limitation of having a small number of neonates relative to the number of features by leveraging a sparse combination of features. Statistical analysis revealed the contribution of myelination and FCs was in agreement with the previous studies. Moreover, the relation between myelination and previously reported FC of some perisylvian sub-regions was demonstrated using hybrid S-F markers. Further studies may explore nonlinear or asynchronous relationships between structure and function. The potential and application of hybrid S-F markers may be the other topic of future studies in diagnostics and prognostics of brain disorders.

Authors' contributions:

R. Namiranian designed and performed the pipeline, and analyzed the data consultation with H. Abrishami Moghaddam, A. Khadem. A. Chalechale assisted with functional analysis and FC extraction. R. Namiranian drafted and H. Abrishami Moghaddam, A. Khadem, and R. Jafari critically revised the work.

References

1. Gao W, Zhu H, Giovanello KS, Smith JK, Shen D, Gilmore JH, et al. Evidence on the emergence of the brain's default network from 2-week-old to 2-year-old healthy pediatric subjects. Proceedings of the National Academy of Sciences. 2009;106(16):6790–5.
2. Knickmeyer RC, Gouttard S, Kang C, Evans D, Wilber K, Smith JK, et al. A structural MRI study of human brain development from birth to 2 years. Journal of neuroscience. 2008;28(47):12176–82.
3. Nelson III CA, Zeanah CH, Fox NA, Marshall PJ, Smyke AT, Guthrie D. Cognitive recovery in socially deprived young children: The Bucharest Early Intervention Project. Science (1979). 2007;318(5858):1937–40.
4. Rathbone R, Counsell SJ, Kapellou O, Dyet L, Kennea N, Hajnal J, et al. Perinatal cortical growth and childhood neurocognitive abilities. Neurology. 2011;77(16):1510–7.
5. Gilmore JH, Knickmeyer RC, Gao W. Imaging structural and functional brain development in early childhood. Nat Rev Neurosci. 2018;19(3):123.
6. Gabrieli JDE, Ghosh SS, Whitfield-Gabrieli S. Prediction as a humanitarian and pragmatic contribution from human cognitive neuroscience. Neuron. 2015;85(1):11–26.
7. Prastawa M, Gilmore JH, Lin W, Gerig G. Automatic segmentation of MR images of the developing newborn brain. Med Image Anal. 2005;9(5):457–66.
8. Dubois J, Alison M, Counsell SJ, Hertz-Pannier L, Hüppi PS, Benders MJNL. MRI of the neonatal brain: a review of methodological challenges and neuroscientific advances. Journal of Magnetic Resonance Imaging. 2021;53(5):1318–43.
9. Edwards AD, Rueckert D, Smith SM, Seada SA, Alansary A, Almalbis J, et al. The Developing Human Connectome Project Neonatal Data Release. Front Neurosci. 2022;16.
10. Larivière S, Vos de Wael R, Hong SJ, Paquola C, Tavakol S, Lowe AJ, et al. Multiscale structure–function gradients in the neonatal connectome. Cerebral Cortex. 2020;30(1):47–58.
11. Li M, Liu T, Xu X, Wen Q, Zhao Z, Dang X, et al. Development of visual cortex in human neonates is selectively modified by postnatal experience. Elife. 2022;11:e78733.
12. Bozek J, Makropoulos A, Schuh A, Fitzgibbon S, Wright R, Glasser MF, et al. Construction of a neonatal cortical surface atlas using Multimodal Surface Matching in the Developing Human Connectome Project. Neuroimage. 2018;179:11–29.
13. Williams LZJ, Fitzgibbon SP, Bozek J, Winkler AM, Dimitrova R, Poppe T, et al. Structural and functional asymmetry of the neonatal cerebral cortex. Nat Hum Behav. 2023;1–14.
14. Zhang S, He Z, Du L, Zhang Y, Yu S, Wang R, et al. Joint analysis of functional and structural connectomes between preterm and term infant brains via canonical correlation analysis with locality preserving projection. Front Neurosci. 2021;1202.
15. O'Muircheartaigh J, Dean III DC, Ginestet CE, Walker L, Waskiewicz N, Lehman K, et al. White matter development and early cognition in babies and toddlers. Hum Brain Mapp. 2014;35(9):4475–87.
16. Daneshvarfard F, Abrishami Moghaddam H, Dehaene-Lambertz G, Kongolo G, Wallois F, Mahmoudzadeh M. Neurodevelopment and asymmetry of auditory-related responses to repetitive syllabic stimuli in preterm neonates based on frequency-domain analysis. Sci Rep. 2019;9(1):10654.
17. Loukas S, Lordier L, Meskaldji D, Filippa M, Sa de Almeida J, Van De Ville D, et al. Musical memories in newborns: A resting-state functional connectivity study. Hum Brain Mapp. 2022;43(2):647–64.

18. Akiyama A, Tsai JD, WY Tam E, Kamino D, Hahn C, Go CY, et al. The effect of music and white noise on electroencephalographic (EEG) functional connectivity in neonates in the neonatal intensive care unit. J Child Neurol. 2021;36(1):38–47.
19. Uchida-Ota M, Arimitsu T, Tsuzuki D, Dan I, Ikeda K, Takahashi T, et al. Maternal speech shapes the cerebral frontotemporal network in neonates: a hemodynamic functional connectivity study. Dev Cogn Neurosci. 2019;39:100701.
20. Tie Y, Rigolo L, Norton IH, Huang RY, Wu W, Orringer D, et al. Defining language networks from resting-state fMRI for surgical planning—A feasibility study. Hum Brain Mapp. 2014;35(3):1018–30.
21. Branco P, Seixas D, Castro SL. Mapping language with resting-state functional magnetic resonance imaging: A study on the functional profile of the language network. Hum Brain Mapp. 2020;41(2):545–60.
22. Minami SB, Oishi N, Watabe T, Uno K, Ogawa K. Auditory related resting state fMRI functional connectivity in tinnitus patients: tinnitus diagnosis performance. Otology & neurotology. 2018;39(1):1–5.
23. Kim S, Knösche TR. Resting state functional connectivity of the ventral auditory pathway in musicians with absolute pitch. Hum Brain Mapp. 2017;38(8):3899–916.
24. Schulte A, Thiel CM, Gieseler A, Tahden M, Colonius H, Rosemann S. Reduced resting state functional connectivity with increasing age-related hearing loss and McGurk susceptibility. Sci Rep. 2020;10(1):1–12.
25. Wang S, Chen B, Yu Y, Yang H, Cui W, Li J, et al. Alterations of structural and functional connectivity in profound sensorineural hearing loss infants within an early sensitive period: A combined DTI and fMRI study. Dev Cogn Neurosci. 2019;38:100654.
26. Xiang HD, Fonteijn HM, Norris DG, Hagoort P. Topographical Functional Connectivity Pattern in the Perisylvian Language Networks. Cerebral Cortex [Internet]. 2010 Mar 1;20(3):549–60. Available from: https://doi.org/10.1093/cercor/bhp119
27. Manning KY, Reynolds JE, Long X, Llera A, Dewey D, Lebel C. Multimodal brain features at 3 years of age and their relationship with pre-reading measures 1 year later. Front Hum Neurosci. 2022;16:965602.
28. Benischek A, Long X, Rohr CS, Bray S, Dewey D, Lebel C. Pre-reading language abilities and the brain's functional reading network in young children. Neuroimage. 2020;217:116903.
29. Reynolds JE, Long X, Grohs MN, Dewey D, Lebel C. Structural and functional asymmetry of the language network emerge in early childhood. Dev Cogn Neurosci. 2019;39:100682.
30. Daneshvarfard F, Moghaddam HA, Kongolo G, Wallois F, Mahmoudzadeh M. Functional and structural correlates of the preterm infant's brain: relating developmental changes of auditory evoked responses to structural maturation. Brain Struct Funct. 2020;1–12.
31. Adibpour P, Lebenberg J, Kabdebon C, Dehaene-Lambertz G, Dubois J. Anatomo-functional correlates of auditory development in infancy. Dev Cogn Neurosci. 2020;42:100752.
32. Adibpour P, Dubois J, Dehaene-Lambertz G. Right but not left hemispheric discrimination of faces in infancy. Nat Hum Behav. 2018;2(1):67–79.
33. Dubois J, Dehaene-lambertz G, Soare C, Cointepas Y, Bihan D Le, Hertz-pannier L. Microstructural Correlates of Infant Functional Development : Example of the Visual Pathways. The Journal of Neuroscience. 2008;28(8):1943–8.
34. Kersbergen KJ, Leroy F, Išgum I, Groenendaal F, de Vries LS, Claessens NHP, et al. Relation between clinical risk factors, early cortical changes, and neurodevelopmental outcome in preterm infants. Neuroimage. 2016;142:301–10.

35. de Vareilles H, Rivière D, Pascucci M, Sun ZY, Fischer C, Leroy F, et al. Exploring the emergence of morphological asymmetries around the brain's Sylvian fissure: a longitudinal study of shape variability in preterm infants. bioRxiv. 2022;
36. Dubois J, Poupon C, Thirion B, Simonnet H, Kulikova S, Leroy F, et al. Exploring the early organization and maturation of linguistic pathways in the human infant brain. Cerebral Cortex. 2016;26(5):2283–98.
37. Dehaene-Lambertz G, Dehaene S, Hertz-Pannier L. Functional neuroimaging of speech perception in infants. Science (1979). 2002;298(5600):2013–5.
38. Mahmoudzadeh M, Dehaene-Lambertz G, Fournier M, Kongolo G, Goudjil S, Dubois J, et al. Syllabic discrimination in premature human infants prior to complete formation of cortical layers. Proceedings of the National Academy of Sciences. 2013;110(12):4846–51.
39. Dehaene-Lambertz G, Montavont A, Jobert A, Allirol L, Dubois J, Hertz-Pannier L, et al. Language or music, mother or Mozart? Structural and environmental influences on infants' language networks. Brain Lang. 2010;114(2):53–65.
40. Shultz S, Vouloumanos A, Bennett RH, Pelphrey K. Neural specialization for speech in the first months of life. Dev Sci. 2014;17(5):766–74.
41. Sprung-Much T, Eichert N, Nolan E, Petrides M. Broca's area and the search for anatomical asymmetry: Commentary and perspectives. Brain Struct Funct. 2022;227(2):441–9.
42. Liu S, Wang H, Song M, Lv L, Cui Y, Liu Y, et al. Linked 4-way multimodal brain differences in schizophrenia in a large Chinese Han population. Schizophr Bull. 2019;45(2):436–49.
43. Kubera KM, Rashidi M, Schmitgen MM, Barth A, Hirjak D, Sambataro F, et al. Structure/function interrelationships in patients with schizophrenia who have persistent auditory verbal hallucinations: A multimodal MRI study using parallel ICA. Prog Neuropsychopharmacol Biol Psychiatry. 2019;93:114–21.
44. Hearne LJ, Lin HY, Sanz-Leon P, Tseng WYI, Gau SSF, Roberts JA, et al. ADHD symptoms map onto noise-driven structure–function decoupling between hub and peripheral brain regions. Mol Psychiatry. 2021;26(8):4036–45.
45. Dubois J, Dehaene-Lambertz G, Kulikova S, Poupon C, Hüppi PS, Hertz-Pannier L. The early development of brain white matter: a review of imaging studies in fetuses, newborns and infants. Neuroscience. 2014;276:48–71.
46. Hotelling H. Relations between two sets of variates. 1936. Biometrika. :321–77.
47. Hughes EJ, Winchman T, Padormo F, Teixeira R, Wurie J, Sharma M, et al. A dedicated neonatal brain imaging system. Magn Reson Med. 2017;78(2):794–804.
48. Makropoulos A, Robinson EC, Schuh A, Wright R, Fitzgibbon S, Bozek J, et al. The developing human connectome project: A minimal processing pipeline for neonatal cortical surface reconstruction. Neuroimage. 2018;173:88–112.
49. Zhu K, Dougherty RF, Wu H, Middione MJ, Takahashi AM, Zhang T, et al. Hybrid-space SENSE reconstruction for simultaneous multi-slice MRI. IEEE Trans Med Imaging. 2016;35(8):1824–36.
50. Fitzgibbon SP, Harrison SJ, Jenkinson M, Baxter L, Robinson EC, Bastiani M, et al. The developing Human Connectome Project (dHCP) automated resting-state functional processing framework for newborn infants. Neuroimage. 2020;223:117303.
51. Shi F, Yap PT, Wu G, Jia H, Gilmore JH, Lin W, et al. Infant brain atlases from neonates to 1- and 2-year-olds. PLoS One. 2011;6(4):e18746.
52. Makropoulos A, Gousias IS, Ledig C, Aljabar P, Serag A, Hajnal J V, et al. Automatic whole brain MRI segmentation of the developing neonatal brain. IEEE Trans Med Imaging. 2014;33(9):1818–31.

53. Schuh A, Makropoulos A, Wright R, Robinson EC, Tusor N, Steinweg J, et al. A deformable model for the reconstruction of the neonatal cortex. In: 2017 IEEE 14th International Symposium on Biomedical Imaging (ISBI 2017). IEEE; 2017. p. 800–3.
54. Batista-García-Ramó K, Fernández-Verdecia CI. What we know about the brain structure–function relationship. Behavioral Sciences. 2018;8(4):39.
55. Greicius MD, Krasnow B, Reiss AL, Menon V. Functional connectivity in the resting brain: a network analysis of the default mode hypothesis. Proceedings of the National Academy of Sciences. 2003;100(1):253–8.
56. Witten DM, Tibshirani R, Hastie T. A penalized matrix decomposition, with applications to sparse principal components and canonical correlation analysis. Biostatistics. 2009;10(3):515–34.
57. Priya S, Burns MB, Ward T, Mars RAT, Adamowicz B, Lock EF, et al. Identification of shared and disease-specific host gene–microbiome associations across human diseases using multi-omic integration. Nat Microbiol. 2022;1–16.
58. Xia CH, Ma Z, Ciric R, Gu S, Betzel RF, Kaczkurkin AN, et al. Linked dimensions of psychopathology and connectivity in functional brain networks. Nat Commun. 2018;9(1):1–14.
59. Yang Q, Zhang X, Song Y, Liu F, Qin W, Yu C, et al. Stability test of canonical correlation analysis for studying brain-behavior relationships: The effects of subject-to-variable ratios and correlation strengths. Hum Brain Mapp. 2021;42(8):2374–92.
60. White T, Su S, Schmidt M, Kao CY, Sapiro G. The development of gyrification in childhood and adolescence. Brain Cogn. 2010;72(1):36–45.
61. Mueller S, Wang D, Fox MD, Yeo BTT, Sepulcre J, Sabuncu MR, et al. Individual variability in functional connectivity architecture of the human brain. Neuron. 2013;77(3):586–95.
62. Zimmermann J, Ritter P, Shen K, Rothmeier S, Schirner M, McIntosh AR. Structural architecture supports functional organization in the human aging brain at a regionwise and network level. Hum Brain Mapp. 2016;37(7):2645–61.
63. Rudie JD, Brown JA, Beck-Pancer D, Hernandez LM, Dennis EL, Thompson PM, et al. Altered functional and structural brain network organization in autism. Neuroimage Clin. 2013;2:79–94.
64. Jiang H, Zhu R, Tian S, Wang H, Chen Z, Wang X, et al. Structural–functional decoupling predicts suicide attempts in bipolar disorder patients with a current major depressive episode. Neuropsychopharmacology. 2020;45(10):1735–42.
65. Wen H, Liu Y, Zhang J, Peng Y, He H. Altered structural-functional coupling of large-scale brain networks in early Tourette syndrome children. In: Medical Imaging 2018: Biomedical Applications in Molecular, Structural, and Functional Imaging. International Society for Optics and Photonics; 2018. p. 1057828.
66. Ball G, Seidlitz J, O'Muircheartaigh J, Dimitrova R, Fenchel D, Makropoulos A, et al. Cortical morphology at birth reflects spatiotemporal patterns of gene expression in the fetal human brain. PLoS Biol. 2020;18(11):e3000976.
67. Van Den Heuvel MP, Kersbergen KJ, De Reus MA, Keunen K, Kahn RS, Groenendaal F, et al. The neonatal connectome during preterm brain development. Cerebral Cortex. 2015;25(9):3000–13.
68. Dubois J, Hertz-Pannier L, Dehaene-Lambertz G, Cointepas Y, Le Bihan D. Assessment of the early organization and maturation of infants' cerebral white matter fiber bundles: a feasibility study using quantitative diffusion tensor imaging and tractography. Neuroimage. 2006;30(4):1121–32.
69. Perani D, Saccuman MC, Scifo P, Anwander A, Spada D, Baldoli C, et al. Neural language networks at birth. Proceedings of the National Academy of Sciences. 2011;108(38):16056–61.

70. Imada T, Zhang Y, Cheour M, Taulu S, Ahonen A, Kuhl PK. Infant speech perception activates Broca's area: a developmental magnetoencephalography study. Neuroreport. 2006;17(10):957–62.
71. Fitzhugh MC, Hemesath A, Schaefer SY, Baxter LC, Rogalsky C. Functional connectivity of Heschl's gyrus associated with age-related hearing loss: a resting-state fMRI study. Front Psychol. 2019;10:2485.
72. Peelle JE. Listening effort: How the cognitive consequences of acoustic challenge are reflected in brain and behavior. Ear Hear. 2018;39(2):204.
73. Erb J, Obleser J. Upregulation of cognitive control networks in older adults' speech comprehension. Front Syst Neurosci. 2013;7:116.
74. Seeley WW, Menon V, Schatzberg AF, Keller J, Glover GH, Kenna H, et al. Dissociable intrinsic connectivity networks for salience processing and executive control. Journal of Neuroscience. 2007;27(9):2349–56.
75. Seeley WW. The salience network: a neural system for perceiving and responding to homeostatic demands. Journal of Neuroscience. 2019;39(50):9878–82.
76. De Asis-Cruz J, Bouyssi-Kobar M, Evangelou I, Vezina G, Limperopoulos C. Functional properties of resting state networks in healthy full-term newborns. Sci Rep. 2015;5(1):17755.
77. Lordier L, Meskaldji DE, Grouiller F, Pittet MP, Vollenweider A, Vasung L, et al. Music in premature infants enhances high-level cognitive brain networks. Proc Natl Acad Sci U S A. 2019;116(24):12103–8.
78. Spann MN, Bansal R, Rosen TS, Peterson BS. Morphological features of the neonatal brain support development of subsequent cognitive, language, and motor abilities. Hum Brain Mapp. 2014;35(9):4459–74.
79. Gossmann A, Zille P, Calhoun V, Wang YP. FDR-corrected sparse canonical correlation analysis with applications to imaging genomics. IEEE Trans Med Imaging. 2018;37(8):1761–74.
80. Ruigrok AN V, Salimi-Khorshidi G, Lai MC, Baron-Cohen S, Lombardo M V, Tait RJ, et al. A meta-analysis of sex differences in human brain structure. Neurosci Biobehav Rev. 2014;39:34–50.
81. Lyall AE, Shi F, Geng X, Woolson S, Li G, Wang L, et al. Dynamic development of regional cortical thickness and surface area in early childhood. Cerebral cortex. 2015;25(8):2204–12.
82. Raznahan A, Shaw P, Lalonde F, Stockman M, Wallace GL, Greenstein D, et al. How does your cortex grow? Journal of Neuroscience. 2011;31(19):7174–7.
83. Ducharme S, Albaugh MD, Nguyen TV, Hudziak JJ, Mateos-Pérez JM, Labbe A, et al. Trajectories of cortical thickness maturation in normal brain development—The importance of quality control procedures. Neuroimage. 2016;125:267–79.
84. Li G, Wang L, Shi F, Lyall AE, Lin W, Gilmore JH, et al. Mapping longitudinal development of local cortical gyrification in infants from birth to 2 years of age. Journal of Neuroscience. 2014;34(12):4228–38.
85. Qiu A, Fortier M V, Bai J, Zhang X, Chong YS, Kwek K, et al. Morphology and microstructure of subcortical structures at birth: a large-scale Asian neonatal neuroimaging study. Neuroimage. 2013;65:315–23.
86. Knickmeyer RC, Wang J, Zhu H, Geng X, Woolson S, Hamer RM, et al. Impact of sex and gonadal steroids on neonatal brain structure. Cerebral cortex. 2014;24(10):2721–31.
87. Knickmeyer RC, Xia K, Lu Z, Ahn M, Jha SC, Zou F, et al. Impact of demographic and obstetric factors on infant brain volumes: a population neuroscience study. Cerebral Cortex. 2017;27(12):5616–25.

88. Gao J, Fetit A, Cupitt J, Passerat-Palmbach J, Alansary AM, Makropoulos A, et al. Sex Differences across Brain Regions in Neonates.
89. Vasung L, Rollins CK, Yun HJ, Velasco-Annis C, Zhang J, Wagstyl K, et al. Quantitative in vivo MRI assessment of structural asymmetries and sexual dimorphism of transient fetal compartments in the human brain. Cerebral Cortex. 2020;30(3):1752–67.
90. Holland D, Chang L, Ernst TM, Curran M, Buchthal SD, Alicata D, et al. Structural growth trajectories and rates of change in the first 3 months of infant brain development. JAMA Neurol. 2014;71(10):1266–74.
91. Tanaka C, Matsui M, Uematsu A, Noguchi K, Miyawaki T. Developmental trajectories of the fronto-temporal lobes from infancy to early adulthood in healthy individuals. Dev Neurosci. 2013;34(6):477–87.
92. Wheelock MD, Hect JL, Hernandez-Andrade E, Hassan SS, Romero R, Eggebrecht AT, et al. Sex differences in functional connectivity during fetal brain development. Dev Cogn Neurosci. 2019;36:100632.
93. Cook KM, De Asis-Cruz J, Lopez C, Quistorff J, Kapse K, Andersen N, et al. Robust sex differences in functional brain connectivity are present in utero. Cerebral Cortex. 2023;33(6):2441–54.
94. Eyre M, Fitzgibbon SP, Ciarrusta J, Cordero-Grande L, Price AN, Poppe T, et al. The Developing Human Connectome Project: typical and disrupted perinatal functional connectivity. Brain. 2021;144(7):2199–213.
95. Zhang L, Wang L, Gao J, Risacher SL, Yan J, Li G, et al. Deep fusion of brain structure-function in mild cognitive impairment. Med Image Anal. 2021;72:102082.
96. Zhang L, Wang L, Zhu D, Initiative ADN. Predicting brain structural network using functional connectivity. Med Image Anal. 2022;79:102463.
97. Rosselli M, Ardila A, Matute E, Vélez-Uribe I. Language development across the life span: A neuropsychological/neuroimaging perspective. Neurosci J. 2014;2014.
98. Dubois J, Dehaene-Lambertz G. Fetal and postnatal development of the cortex: MRI and genetics. 2015.
99. Chi JG, Dooling EC, Gilles FH. Gyral development of the human brain. Annals of Neurology: Official Journal of the American Neurological Association and the Child Neurology Society. 1977;1(1):86–93.
100. Li G, Nie J, Wang L, Shi F, Lyall AE, Lin W, et al. Mapping longitudinal hemispheric structural asymmetries of the human cerebral cortex from birth to 2 years of age. Cerebral cortex. 2014;24(5):1289–300.